A Triaxial Permeameter to Study the Mechanical Consequences of Internal Erosion

Sara Ataii, Jonathan Fannin
Department of Civil Engineering– University of British Columbia, Vancouver, BC, Canada

GeoCalgary 2022 October 2-5 Reflection on Resources

ABSTRACT
Internal erosion is believed to account for about half of all embankment dam failures and deficiency investigations. In managing the risk, there is a need to advance from current empirical methods of assessment to a mechanics-based understanding of the erosion phenomena. A triaxial permeameter was designed and commissioned to obtain data for Bennett South Moraine sand within the critical state framework. In the triaxial permeameter testing, the reconstituted specimen is subject to downward seepage flow prior to shearing. Any mass loss and volume change of the specimen are monitored in real-time during seepage. Custom features of the newly developed triaxial permeameter are described with specific reference to (i) seepage control system, (ii) inflow boundary end-platen (of the top cap), (iii) outflow boundary end-platen (of the base pedestal), (iv) double-walled triaxial cell and (v) mass loss measurement unit. Experience gained in commissioning the device to impose multistage seepage flow, whilst monitoring the specimen response, is reported.

RÉSUMÉ
On pense que l'érosion interne est à l'origine d'environ la moitié de toutes les ruptures de barrages en remblai et des enquêtes sur les carences. Dans la gestion du risque, il est nécessaire de passer des méthodes d'évaluation empiriques actuelles à une compréhension mécanique des phénomènes d'érosion. Un perméamètre triaxial a été conçu et mis en service pour obtenir des données sur le sable de Bennett South Moraine dans le cadre de l'état critique. Dans l'essai au perméamètre triaxial, l'échantillon reconstitué est soumis à un flux d'infiltration vers le bas avant le cisaillement. Toute perte de masse et tout changement de volume de l'échantillon sont surveillés en temps réel pendant l'infiltration. Les caractéristiques personnalisées du perméamètre triaxial nouvellement développé sont décrites avec une référence spécifique au (i) système de contrôle des infiltrations, (ii) plateau d'extrémité de limite d'entrée (du capuchon supérieur), (iii) plateau d'extrémité de limite de sortie (du socle de base) , (iv) cellule triaxiale à double paroi et (v) unité de mesure de perte de masse. L'expérience acquise dans la mise en service du dispositif pour imposer un flux d'infiltration à plusieurs étages, tout en surveillant la réponse de l'échantillon, est rapportée.

1 INTRODUCTION

The movement of particles with seepage flow in soil, termed internal erosion, governs about half of all embankment dam failures (ICOLD, 2017). The growing need for improvements to managing this risk is advancing developments beyond simple empirical assessment methods towards a mechanics-based understanding of the phenomenon. In doing so, the findings of triaxial permeameter tests are being used to inform on the mechanical consequences of internal erosion (see for example Chang et al., 2014; Ke and Takahashi, 2014; Mehdizadeh et al., 2017; Li et al., 2020). A triaxial permeameter test includes four stages: specimen reconstitution, consolidation, seepage, and axial loading in compression. Internal erosion takes place during the seepage stage and the mechanical response of the eroded specimen is characterized by shearing it.

The erosion response of a specimen under seepage can be characterized as suffusion or suffosion with respect to mass loss, volume change, and change in the hydraulic conductivity of the specimen (Fannin and Slangen, 2014; USBR, 2019). Suffusion is defined as “seepage-induced mass loss without a change in volume, accompanied by an increase of hydraulic conductivity”; In contrast, suffosion is “seepage-induced mass loss accompanied by a reduction in volume and a change in hydraulic conductivity”.

The UBC triaxial permeameter was designed and commissioned to study the mechanical consequences of internal erosion for ideally gap-graded gradations of Bennett South Moraine sand. It represents a further and innovative development of the triaxial test device reported by McClelland (2020). The objectives of this paper are: (i) to describe the seepage-relevant features of the UBC triaxial permeameter, (ii) to demonstrate its capacity for monitoring the hydromechanical response of the specimen under seepage, and (iii) to characterize the erosion response of a test within the suffusion/suffosion framework.

2 UBC TRIAXIAL PERMEAMETER

The UBC triaxial permeameter (TXP) is capable of running both triaxial and triaxial permeameter types of tests. Thus, its seepage-relevant features alongside all the features of a conventional triaxial device, allow for performing triaxial permeameter tests. Fig. 1 shows a generic view of the device while running a triaxial permeameter test. In the following, seepage-relevant features of the device are described.

2.1 Seepage Control System

To erode the specimen in a triaxial permeameter test, the specimen is subjected to a hydraulic demand using the seepage control system. The demand can either be

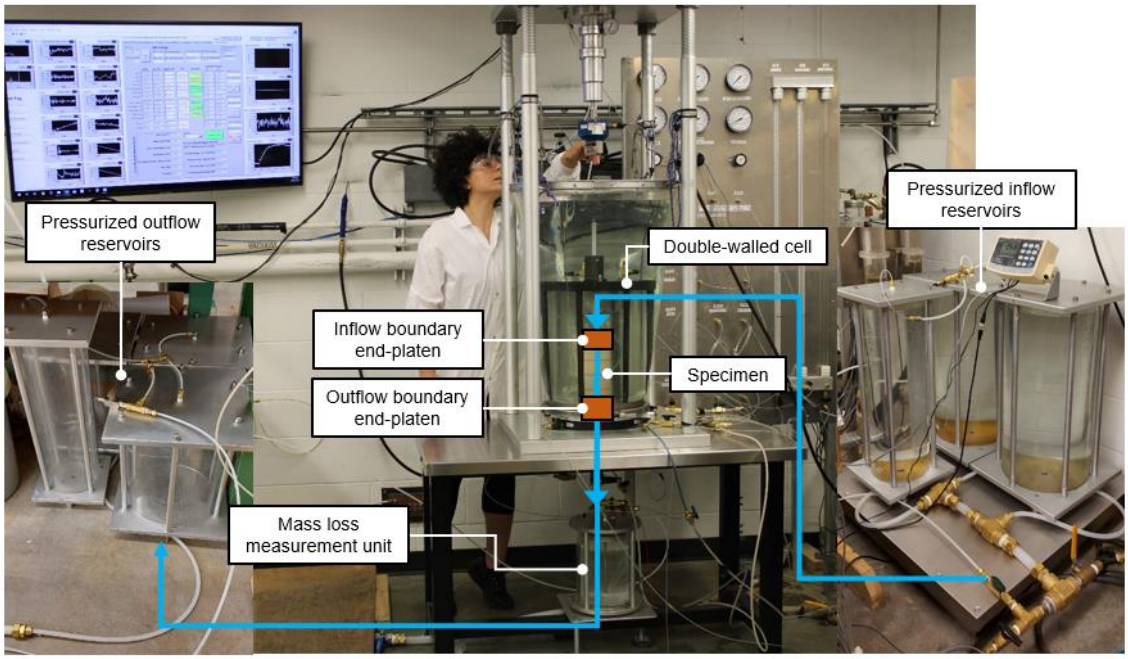

Figure 1. Generic view of UBC triaxial permeameter

differential head across the specimen or flow. In a head-controlled seepage system, the differential head across the specimen is held constant and the induced flow rate is measured. In contrast, in a flow-controlled seepage system, the specimen is subjected to a constant flow rate and the induced differential head across the specimen is monitored. Both systems were used in previous triaxial permeameter studies (see Table 1).

The seepage control system of the UBC triaxial permeameter is head-controlled and includes: (a) pressurized inflow reservoirs that connect to the inflow end-platen, (b) a scale beneath the inflow reservoirs to measure flow rate by continuously measuring the amount of mass that enters the system (c) a differential pressure transducer measuring the differential head across the specimen (Δh[1] = h_i[2] – h_o[3]), and (d) pressurized outflow reservoirs connecting to the outflow end-platen (see Fig. 2). Pressure on the outflow reservoir (i.e. h_o) is kept constant. While monitoring the differential pressure across the specimen, the inflow reservoir pressure is increased to reach the desired hydraulic gradient and then, in a feedback control-loop, it is continuously adjusted to hold the hydraulic gradient constant. The seepage control system is capable of applying hydraulic gradients up to a maximum value of 25 with a resolution of ±0.02.

2.2 Inflow Boundary End-Platen

Inflow boundary end-platen in downward triaxial permeameter testing (top cap) has a seepage-relevant function of introducing uniform flow to the specimen. Adverse non-uniformities in the exiting flow profile from the top cap may control the erosion response of the specimen. Top caps used in previous triaxial permeameters were usually comprised of a single inlet port, a permeable layer to distribute the flow from the inlet, and a perforated plate (see Table 1).

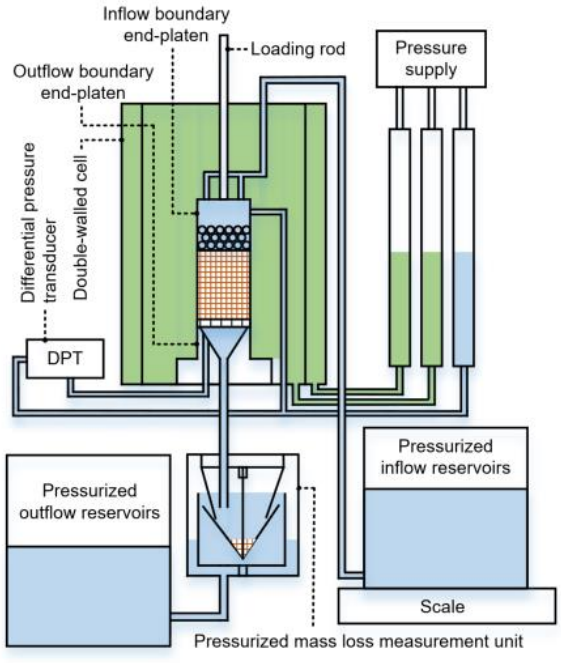

Figure 2. Schematic diagram of UBC triaxial permeameter

[1] Differential pressure across the specimen
[2] Pore water pressure on the inflow
[3] Pore water pressure on the outflow

The UBC triaxial permeameter has a custom-designed top cap consisting of (1) two primary inlet ports that yield four secondary inlet ports; (2) a flow-conditioning chamber; (3) a rigid perforated plate (opening size: 0.8 mm, open area: 20%); (4) a fine wire mesh (#200) in contact with the specimen, and (5) a location of pore water pressure measurement at the center of the primary perforated plate. The flow-conditioning chamber comprises an upper hollow chamber, and a lower chamber filled with three layers of 9-mm diameter glass beads (see Fig. 3).

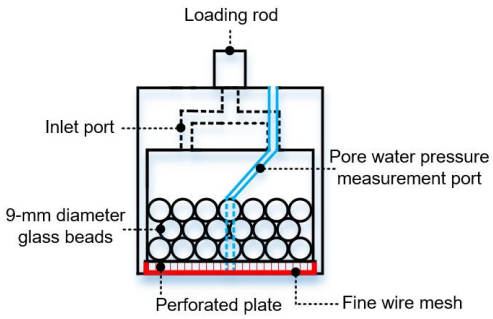

Figure 3. Inflow boundary end-platen configuration of UBC triaxial permeameter

The hydraulic performance of the top cap was studied in an experimental parametric study and proved to be satisfactory for the application of this study (Ataii and Fannin, 2019). A combination of three different hydraulic mechanisms that occur within the flow conditioning chamber, identified as spreading, mixing, and dispersion, are responsible for the uniformity of the exiting flow profile from the top cap.

2.3 Outflow Boundary End-Platen

The seepage-relevant function of outflow boundary end-platen in downward triaxial permeameter testing (base pedestal) is to allow for unimpeded movement of eroded particles out of the specimen. The general configuration of base pedestals in previous triaxial permeameters usually includes a relatively open surface in contact with the bottom of the specimen, supported on a hollow funnel-shaped base pedestal to facilitate the downward movement of eroded particles (see Table 1).

The outflow boundary end-platen of the UBC triaxial permeameter is configured with a wire mesh in contact with the specimen, a rigid perforated plate under the wire mesh to provide strength for load transfer, a funnel-shaped hollow base pedestal, and a port for measuring the pore water pressure at the bottom of the specimen as depicted in Fig. 4.

The most important feature of the outflow boundary end-platen is its opening characteristics that are conditioned by opening size and percentage open area. For the ideally gap-graded materials of interest in this study (see section 3), the opening characteristics were selected to provide the maximum ease of outward movement of any finer fraction content (with d_{100} = 0.2 mm) while preventing erosion of the coarser fraction (with d_0 = 1.4 mm). The selected mesh has an opening size of 1.37 mm and a percentage open area of 73%. Fig. 5 shows parts of inflow and outflow boundary end-platens that are in contact with the specimen.

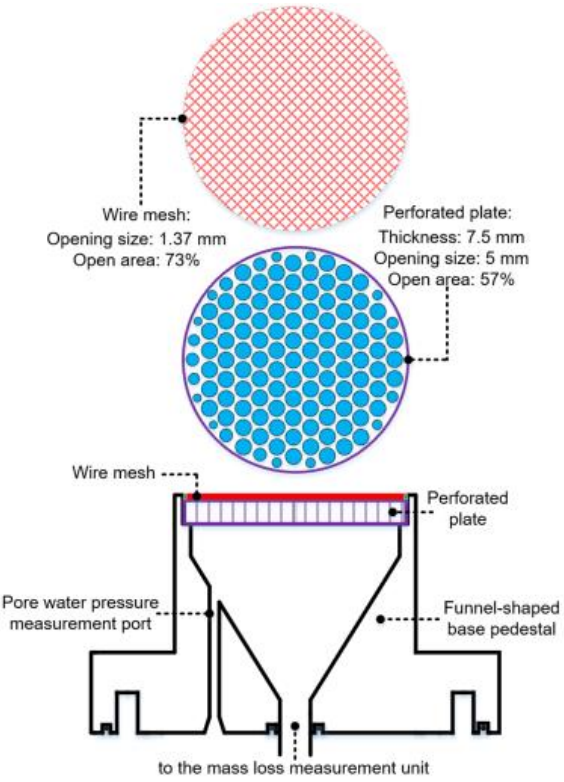

Figure 4. Outflow boundary end-platen configuration of UBC triaxial permeameter

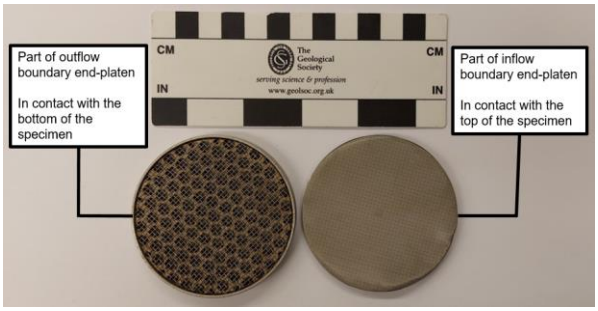

Figure 5. Parts of inflow and outflow boundary end-platens in contact with the specimen

2.4 Double-Walled Triaxial Cell

The double-walled cell, from an earlier flexible wall permeameter device (Slangen, 2015), accommodates reconstituting a cylindrical specimen with 75 mm diameter and 150 mm height against inflow and outflow boundary end-platens, application of cell pressure, and measurement of volume change during the seepage stage.

During the stage of seepage flow, the specimen is an open system. Water enters the specimen through the top cap, and leaves it through the base pedestal. Thus, it is not possible to measure any specimen volume change by directly measuring the volume of water that goes in/out of the specimen through the drainage line (the conventional method of measuring volume change by burette in triaxial tests). In most of the previous studies, volume change in the seepage stage was monitored by combining independent measurements of lateral and vertical deformations using a variety of methods for capturing the lateral deformation (see Table 1).

The use of a double-walled cell for measuring volume change originated in unsaturated soil mechanics where again it is not possible to measure volume change using the conventional method. Implementing this method, the inner and outer cells are filled and saturated with de-aired water and are kept under the same pressure throughout the test. The presence of the outer cell ensures an equal pressure on either side of the inner cell and thus eliminates any deformation that would otherwise occur due to a differential pressure across it. Any volume change experienced by the specimen induces an equal change in the volume of the cell fluid (de-aired water) surrounding the specimen: it is measured through a burette connected to the inner cell. The accuracy of volume change measurement by this method in the current study is ±0.05 cm^3 (0.01% of the specimen volume) and the capacity is 100 cm^3.

2.5 Mass Loss Measurement During Seepage

Any eroded mass is collected and measured using a method adapted from Ke and Takahashi (2014). The discharge water with eroded finer fraction particles flows into a pressurized mass loss measurement unit (MLMU) through a connecting pipe from the base pedestal. The pressure in the MLMU equals the (back) pressure on the outflow reservoirs and the bottom of the specimen and it is kept constant throughout the seepage stage.

Inside the MLMU, a conical-shaped funnel, connected to a miniature load cell, is submerged in a cylinder filled with water (see Fig. 6). As flow from the base pedestal exits the pipe its velocity decreases because of the increased effective area. A combination of flow velocity reduction, gravity, and the shape of the funnel yield settlement of the eroded particles and overflow of water from the edges of the inner cylinder. The submerged weight of eroded particles is continuously measured by the miniature load cell. Resolution and capacity of measurement are 2 g and 1000 g respectively. The overflow water drains to the pressurized outflow reservoirs. This eliminates the pressure disturbance induced by the frequent opening and closing of the solenoid valve in the original design of Ke and Takahashi (2014).

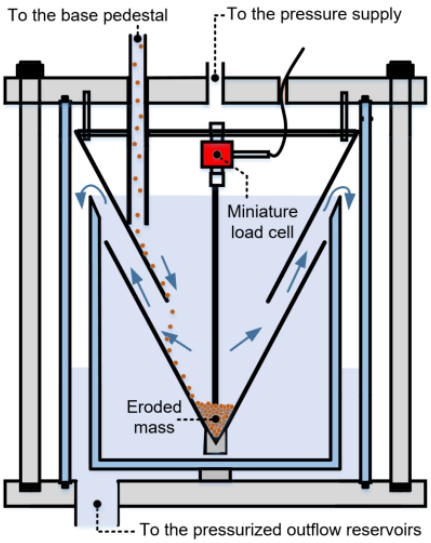

Figure 6. Mass loss measurement unit of the UBC triaxial permeameter

3 TEST MATERIALS

Uniformly-graded fractions of sand-sized materials from Bennett South Moraine borrow source (BSM sand) of kame moraine are used to form an ideally gap-graded gradation that is susceptible to internal erosion. BSM sand is an

Table 1. Overview of select triaxial permeameter features

Reference	Seepage control system	Inflow boundary configuration	Outflow boundary configuration	Volume change measurement	Mass loss measurement
Chang and Zhang (2014)	Head	Highly permeable filter +perforated plate + fine wire mesh	Hollow base pedestal + perforated plate + rigid mesh or geotextile	LVDT + photographic	Manual & discrete
Ke and Takahashi (2014)	Flow	Funnel-shaped top cap + perforated plate	Hollow base pedestal + perforated plate	LVDT + clip gages	Automated & continuous
Mehdizadeh et al. (2017)	Flow	Glass spheres + perforated plate + fine wire mesh	Hollow base pedestal + netted plate + rigid mesh	LVDT + photogrammetry	Automated & continuous
Li et al. (2020)	Head	Funnel-shaped top cap + perforated plate	Funnel-shaped base pedestal + perforated plate	Cell fluid	Manual & discrete
Current study (2022)	Head	Hollow chamber + glass beads + perforated plate + fine wire mesh	Hollow base pedestal + perforated plate + wire mesh	Double-walled triaxial cell	Automated & continuous

angular to sub-angular sand with a predominately siliceous mineralogy that includes a significant percentage of carbonates.

A uniformly-graded fraction, termed BSM-6/14, provides the coarser fraction and BSM-70/140 provides the finer fraction. The two fractions are mixed to form a gap-graded mixture with $D_{15}'/d_{85}' = 9.4$ and finer fraction content S_f = 20% that is termed BSM-10:20 in the current study (see Fig. 7).

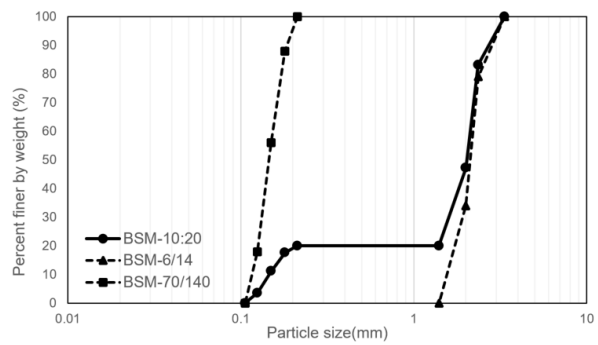

Figure 7. Particle size distribution of the tested gradation and its fractions

4 TEST PROCEDURE

The test specimen is reconstituted to a target loose void ratio using the moist tamping technique by under compaction (Ladd, 1978). Thereafter it is back-percolated with de-aired water, saturated by back-pressuring, and isotropically consolidated to a target mean effective stress (p_c'). Upon completion of consolidation, the specimen is subjected to multistage downward seepage flow. More specifically, the imposed hydraulic demand includes a small initial hydraulic gradient that is stepwise increased to a maximum value and then decreased to a condition of no-flow in a single step. In the final stage of the test, under desired drainage conditions (drained/undrained), the eroded specimen is subjected to axial compression at a displacement rate of 0.25 mm/min to an end-of-test axial strain of about 25%.

5 ILLUSTRATIVE SEEPAGE RESPONSE

A specimen of BSM-10:20 gradation was reconstituted to a loose state and isotropically consolidated to p' = 50 kPa. Upon completion of the consolidation, hydraulic demand was applied to the specimen by increasing the hydraulic gradient in six increments to a maximum value i_{max} = 1.6 (yielding i = 0.2, 0.4, 0.6, 0.8, 1, and 1.6) and decreasing it to zero in a single gradual step (see Fig. 8a). The minimum duration of each step was 5 minutes to obtain a reliable measure of hydraulic conductivity value (± 0.01 cm/s): step durations longer than 5 minutes were informed by the erosion response of the specimen.

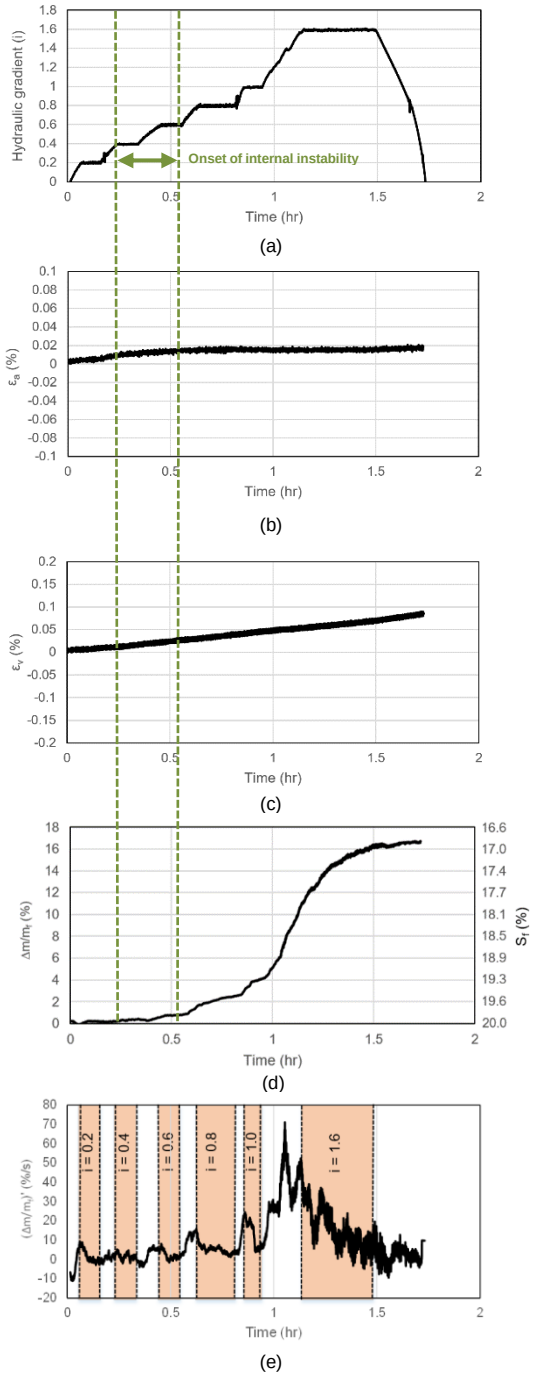

Figure 8. Seepage narrative with respect to time: (a) hydraulic demand, (b) variation of axial strain, (c) variation of volumetric strain, (d) erosion response in terms of percent finer fraction loss, and (e) variation of rate of percent finer fraction loss

The erosion response of the specimen in terms of axial and volumetric strains is shown in Fig. 8b and 8c. The specimen exhibited compressive axial strain that developed mostly from i = 0.4 to i = 0.6, and to a maximum of $\varepsilon_{a,max}$ = 0.02%. Likewise, contractive volumetric strain

developed through to a $\varepsilon_{v,max}$ = 0.1%. The small values of maximum axial and volumetric strain that the specimen experienced under the influence of seepage flow are considered negligible and are not believed to be associated with any significant rearrangement of particles contributing to the load transfer.

Fig. 8d shows the evolution of mass loss in terms of percentage finer fraction loss ($\Delta m/m_f$) and finer fraction content (S_f) with time. The percent finer fraction loss is calculated based as follows:

$$\Delta m/m_f\,(\%) = \frac{\text{eroded mass}}{\text{the initial mass of finer fraction}} * 100 \qquad [1]$$

Mass loss started at a hydraulic gradient of about 0.4 and amounted to about 1 % of the finer fraction content at i = 0.6. Thereafter, mass loss increased gradually with increasing hydraulic gradient to 16% at i_{max} = 1.6. No significant mass loss occurred during the removal of hydraulic demand and commensurate reduction in seepage flow to zero. As a result, the finer fraction content of the specimen diminished from S_f = 20% at the start of seepage to S_f = 16.9% at the end. To verify the performance of the mass loss measurement unit, the accumulated eroded mass was collected after the test, oven-dried, and weighed. The difference between the end-of-seepage recorded mass loss using the real-time MLMU data acquisition system and the post-test collected amount was found to be smaller than the measurement resolution of the unit (2 g). Fig. 8e provides an analysis of the response depicted in Fig. 8d, and shows how the slope of $\Delta m/m_f$ - time graph changed over time (i.e. the variation in rate of percent finer fraction loss $(\Delta m/m_f)'$ with time). At a constant hydraulic gradient, although $(\Delta m/m)'$ varied with time, the general trend is one of a constant value or decrease. In contrast $(\Delta m/m)'$ generally increased while an increment hydraulic gradient was being applied.

The erosion response of the specimen in terms of change in hydraulic conductivity is shown in Fig. 9. The initial hydraulic conductivity k_i = 0.23 (± 0.01) cm/s at i = 0.2. It remained almost constant between i = 0.2 and i = 0.4 and decreased to k_{min} = 0.21 at i = 0.4. Thereafter, the hydraulic conductivity increased linearly with increasing hydraulic gradient to i = 0.6. For two increments of hydraulic gradient with longer duration (i = 0.8 and i = 1.6), the hydraulic conductivity increased within the step which is attributed to action of finer fraction mass loss. Over the course of multi-stage seepage flow, the hydraulic conductivity increased to a value of k_l = 0.36 cm/s.

According to the Fannin and Slangen (2014) definition of suffusion as “seepage-induced mass loss without a change in volume, accompanied by an increase of hydraulic conductivity”, the response of the BSM-10:20 gradation to multi-stage seepage flow (in Fig. 8 and Fig. 9) is suffusive. It appears the onset of internal instability was triggered at $0.4 \le i_c \le 0.6$.

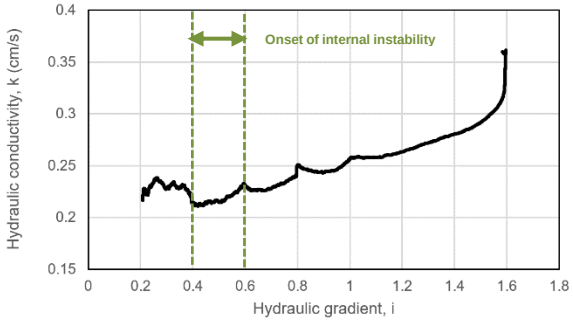

Figure 9. Variation of hydraulic conductivity with hydraulic gradient

6 DISCUSSION

In this section, key attributes of the BSM-10:20 gradation response reported herein are compared with those reported in a previous study (Slangen, 2015) on a different gradation of gap-graded soil from the same borrow source (see Table 2).

Slangen studied the erosion response of a slurry deposited specimen of similar but not identical gap-gradation, using a flexible wall permeameter that imposed upward flow. The device could not measure mass loss from the specimen. Based on an interpretation of no axial strain and negligible volumetric strain, the erosion response was characterized as suffusive with the onset of internal instability at i_c = 0.3. In the absence of mass loss measurement, the onset of internal instability was identified from a change in hydraulic conductivity. The order of magnitude difference in values of hydraulic conductivity (see Table 2) is attributed to the difference in the macrostructure of the moist-tamped specimens of the current study and slurry-deposited specimens of Slangen (2015).

Observed similarities between the two studies are the suffusive nature of the specimen response, and the relatively smaller magnitude of the hydraulic gradient to trigger instability with upward flow, which is to be generally expected based on theory (see Li and Fannin, 2022). Experience from the current study suggests that whilst a measurement of volume change (if any) and hydraulic conductivity inform on the erosion response, the real-time mass loss measurement is very instructive for a confident interpretation of the specimen response.

Table 2. Summary of key attributes of compared tests

Reference	Reconstitution technique	D_{15}'/d_{85}'	S_{fi} (%)	P_c' (kPa)	Seepage direction	k_i (cm/s)	i_c	k_l (cm/s)	S_{fe} (%)	$\varepsilon_{a,max}$ (%)	$\varepsilon_{v,max}$ (%)	Erosion response
Slangen (2015)	Slurry deposition	10.4	25	53	Upward	0.019	0.3	0.013	NA	0.00	0.72	Suffusion
Current study (2022)	Moist tamping	9.4	20	50	Downward	0.23	0.4-0.6	0.36	16.9	0.02	0.1	Suffusion

7 SUMMARY REMARKS

To better understand the mechanical consequences of internal erosion phenomena, it is essential to study the mechanical response of eroded gradations through axial compression to shear the test specimen.

Custom features of the newly developed triaxial permeameter (TXP) include: (i) seepage control system, (ii) inflow boundary end-platen (of the top cap), (iii) outflow boundary end-platen (of the base pedestal), (iv) double-walled triaxial cell and (v) mass loss measurement unit are described.

The seepage response of a moist tamped gap-graded sand using the TXP device is described and compared to a slurry deposited specimen of the same soil type. The results of the comparison highlight the importance of real-time mass loss measurement for the interpretation of erosion response.

REFERENCES

Ataii, S. and Fannin, J., 2019, June. EWG-23 Inflow Boundary Conditions in Triaxial Permeameter Testing. In Book of Abstracts (p. 74).

Chang, D., Zhang, L. and Cheuk, J., 2014. Mechanical consequences of internal soil erosion. HKIE Transactions, 21(4), pp.198-208.

Fannin, R.J. and Slangen, P., 2014. On the distinct phenomena of suffusion and suffosion. Géotechnique Letters, 4(4), pp.289-294.

Fannin, R.J., Slangen, P., Mehdizadeh, A., Disfani, M.M., Arulrajah, A. and Evans, R., 2015. Discussion: On the distinct phenomena of suffusion and suffosion. Géotechnique Letters, 5(3), pp.129-130.

ICOLD, 2017. Internal Erosion of Existing Dams, Levees and Dikes, and their Foundations, Bulletin 164, International Commission on Large Dams, Paris, France.

Ke, L. and Takahashi, A., 2014. Triaxial erosion test for evaluation of mechanical consequences of internal erosion. Geotechnical Testing Journal, 37(2), pp.347-364.

Ladd, R.S., 1978. Preparing test specimens using undercompaction. Geotechnical testing journal, 1(1), pp.16-23.

Li, M. and Fannin, R.J., 2022. Internal erosion: critical hydraulic gradient in one-dimensional vertical seepage and its relation to soil gradation. Canadian Geotechnical Journal, 59(5), pp.769-772.

Li, S., Russell, A. and Muir Wood, D., 2020. The influence of particle size distribution homogeneity on the shearing of soils having been subjected to internal erosion. Canadian Geotechnical Journal, (ja).

McClelland, V.A., 2020. On the critical state of gap-graded sandy soil (MASc thesis, University of British Columbia).

Mehdizadeh, A., Disfani, M.M., Evans, R., Arulrajah, A. and Ong, D.E.L., 2017. Mechanical consequences of suffusion on undrained behaviour of a gap-graded cohesionless soil-an experimental approach. Geotechnical Testing Journal, 40(6), pp.1026-1042.

Slangen, P.H.H., 2015. On the influence of effective stress and micro-structure on suffusion and suffosion (Doctoral dissertation, University of British Columbia).

USBR, 2019. Internal Erosion Risks for Embankments and Foundations, Chapter D-6, United States Bureau of Reclamation, Denver, CO.